

VARIATIONS IN DROP-SIZE DISTRIBUTIONS ASSOCIATED WITH THE DEGREE OF BAROCLINICITY OF THE ENVIRONMENT

Karen E. Brugman* and Courtney Schumacher
Texas A&M University, College Station, Texas

1. INTRODUCTION

The microphysical properties of mesoscale precipitation systems can be altered by season, location, storm type, surface temperature, wind shear, etc. This study focuses on microphysical variations of subtropical mesoscale systems in Southeast Texas based on the degree of baroclinicity of the environment. The subtropics are uniquely situated to study synoptic variations since they act as a transition zone between the tropics and mid-latitudes. In the subtropics, baroclinic environments tend to represent extratropical influences whereas barotropic environments better represent tropical influences, and these different influences can potentially affect the dynamics and microphysical processes that occur in mesoscale systems.

Synoptic-scale variability within seasons causes classifications based solely on seasons to break down, e.g., although a more tropical regime is present over Southeast Texas during summer, not all days can be classified as barotropic. This study uses drop-size distributions (DSDs) calculated from a disdrometer to determine variations in microphysical processes in mesoscale rain systems by season and baroclinicity.

2. BAROCLINICITY CLASSIFICATIONS

The degree of environmental baroclinicity is parameterized using NCEP reanalysis daily mean surface temperatures over a 10 x 10 degree grid box centered over Southeast Texas (25°N-35°N and 100°W-90°W). The maximum horizontal temperature gradient over the entire grid was used as the baroclinicity parameter. The maximum temperature difference was calculated by taking the difference between the grid point with the highest temperature and the grid point with the lowest temperature for each day. Results of the calculations were retrieved for one year (June 2004 - May 2005), with temperature differences ranging from 4-35°C. The baroclinicity categories are identified using these maximum difference values, yielding classifications of barotropic, weakly baroclinic and strongly baroclinic for the background environment. Days identified as barotropic range from 0-9°C, weakly baroclinic between 10-19°C, and strongly baroclinic >20°C.

Each day of the 12-month record was assigned a baroclinicity category. There were 161 barotropic, 155

weakly baroclinic, and 49 strongly baroclinic days. The barotropic, weakly baroclinic, and strongly baroclinic environments account for 44.1%, 42.4% and 13.4% of the total occurrences, respectively. Determining the relative importance of each baroclinicity category by season helps to validate the baroclinicity classifications (Table 1). The seasonal statistics demonstrate that, as expected, barotropic days dominate the summer months occurring 89% of the time, and the highest frequency of strongly baroclinic days is in winter with 40% occurrence versus <10% in other seasons. However, there are weakly baroclinic days during every season and they even outnumber strongly baroclinic days in winter. This result suggests that while analyzing the microphysics by season is useful, such a division of data misses the intraseasonal variations captured by the baroclinicity designations.

Table 1 Number of occurrences and percent of total occurrence of each baroclinicity category by season for June 2004 - May 2005.

Season	Barotropic	Weakly Baroclinic	Strongly Baroclinic
JJA 2004	82(89.1%)	10(10.9%)	0 (0.0%)
SON 2004	40(44.0%)	44(48.3%)	7 (7.7%)
DJF 2004-05	8 (8.9%)	46(51.1%)	36(40.0%)
MAM 2005	31(33.7%)	55(59.8%)	6 (6.5%)

3. DISDROMETER DATA

Data from a Joss-Waldvogel disdrometer located in Southeast Texas and in the center of the NCEP grid (~30.7°N, 96.4°W) is available at select intervals from July-December 2004 and continuously from December 16, 2004 through July 31, 2005. The disdrometer measures precipitation drop sizes at 10-second intervals in 20 average diameter bins. It is important to note that although the disdrometer samples drops beginning at diameters of 0.3 mm, there is an under sampling in the four smallest bins up to a diameter of 0.656 mm (see Figs 1-3). Therefore data from these bins will not be considered in the subsequent discussion. For the purpose of analysis, the data was re-binned into 1-minute consecutive intervals. Using a variation of the storm definition of Steiner and Smith (2000), the beginning and end of each storm was identified by a minimum rain rate of 0.1 mmh⁻¹, rain periods separated by breaks lasting less than 4 hours were combined into a single storm, and a minimum storm total rain accumulation of 2.5 mm was required. One-minute samples within the rain period with less than 10 drops were not included to reduce sampling error (Smith et al. 1993).

* *Corresponding author address:* Karen E. Brugman, Texas A&M Univ., Dept. of Atmospheric Science, College Station, TX 77843-3150; kbrugman@tamu.edu

Table 2 Microphysical parameters derived from DSD observations during 30 identified storms from October 2004 through July 2005, including baroclinicity classifications from NCEP data: barotropic (B), weakly baroclinic (W), and strongly baroclinic (S). Shaded rows indicate storms selected for case studies in section 4.1.

Storm	Date	Duration [hh:mm]	a	b	RT [mm]	Max RR [mmh ⁻¹]	Baroclinicity
S01	10/31/04	01:38	400	1.40	4.9	32.0	W
S02	11/01/04	10:23	250	1.34	26.2	55.1	W
S03	11/02/04	04:11	250	1.40	7.0	9.8	S
S04	12/22/04	04:55	350	1.42	9.7	51.8	S
S05	01/02/05	09:21	200	1.36	20.2	46.8	B
S06	01/05/05	01:27	150	1.25	5.5	29.3	W
S07	01/13/05	05:59	375	1.38	24.0	75.4	S
S08	01/27-28/05	19:40	225	1.34	21.9	32.7	W
S09	01/30-31/05	18:39	200	1.36	7.0	33.2	S
S10	02/01-02/05	15:12	300	1.44	11.2	10.8	S
S11	02/06-07/05	06:02	250	1.36	63.8	52.6	W
S12	02/23/05	05:36	350	1.40	9.8	42.0	W
S13	02/24/05	00:40	500	1.40	3.9	28.7	S
S14	02/24/05	06:37	400	1.34	30.0	111.4	S
S15	02/26-27/05	15:18	300	1.60	9.6	3.0	W
S16	03/02/05	07:37	300	1.42	14.3	12.3	W
S17	03/07/05	02:33	275	1.28	5.6	39.2	W
S18	03/19-20/05	03:35	450	1.66	35.3	77.5	W
S19	03/21/05	04:24	400	1.36	9.9	110.4	W
S20	03/27/05	05:19	350	1.42	5.3	5.2	S
S21	04/01/05	01:35	400	1.48	15.1	79.4	W
S22	04/06/05	00:56	400	1.36	21.6	92.6	W
S23	05/29/05	03:19	300	1.40	9.5	45.0	W
S24	07/08/05	02:59	400	1.42	30.1	110.1	B
S25	07/09/05	00:38	350	1.50	11.7	64.6	B
S26	07/14-15/05	10:44	400	1.50	31.7	59.1	B
S27	07/15/05	05:12	300	1.38	6.3	19.2	B
S28	07/16-17/05	07:55	300	1.40	6.9	52.7	B
S29	07/17/05	05:25	250	1.40	10.7	94.2	B
S30	07/18/05	04:04	400	1.55	3.8	70.2	B
Average		07:51	325	1.40	15.8	51.5	

The reflectivity factor, Z , and rain rate, R , were calculated from the DSD for each of the 30 storms identified (Table 2). The Z - R relationship of the form $Z=aR^b$ was then calculated for each storm. The exponent, b , was fit to each data set, while the multiplicative factor, a , was calculated using a fixed value of $b=1.4$, where 1.4 is the mean value of the exponents calculated for the storms. The storm total rain accumulation (RT) and maximum rain rate (RR), as well as the baroclinicity designation derived from the NCEP data are also provided.

4. RESULTS

Understanding the cumulative DSD results begins with a detailed investigation of individual storm distributions from each of the baroclinicity categories. It is then possible to begin drawing larger conclusions from the relationship between the seasonal variations as opposed to those resulting from a specific environmental baroclinicity.

4.1 Case Studies

The following three storms were chosen to represent each of the baroclinicity categories. The storms were chosen based on their similar RT values, allowing for a clearer comparison between the other parameters.

Histograms of the DSDs for these storms are shown in Fig 1. Three distinct peaks are identifiable in the histograms: Peak 1 at 1.116 mm, Peak 2 at 1.912 mm, Peak 3 at 3.198 mm. Steiner and Waldvogel (1987) identified three strong peaks (0.7 mm, 1 mm, 2 mm) and a weak peak (3.2 mm) in a data set spanning a variety of locations. While there is some evidence of an 0.7 mm peak in our observed distributions which varies between the baroclinicity categories. The undersampling discussed in Section 3 creates uncertainty in the magnitude and relative importance of this peak. However, our disdrometer's three peaks coincide with the other peaks in Steiner and Waldvogel. Since the peaks are not necessarily present in each case, the relative heights of the peaks are of primary importance when comparing the distributions.

Barotropic: Storm S25 occurred in July 2005 and lasted 38 minutes with a maximum rain rate of 64.6 mmh⁻¹. The large-scale environment of this system exhibited weak temperature gradients, weak wind shear associated with an offshore low, and thermally force strong convection. Radar shows that the storm was in its mature stage over the disdrometer site. The DSD for this case contains all three peaks. Note that Peaks 1 and 2 are distinct and of similar magnitudes while Peak 3 is hidden amongst the thick tail at the high end of the spectrum.

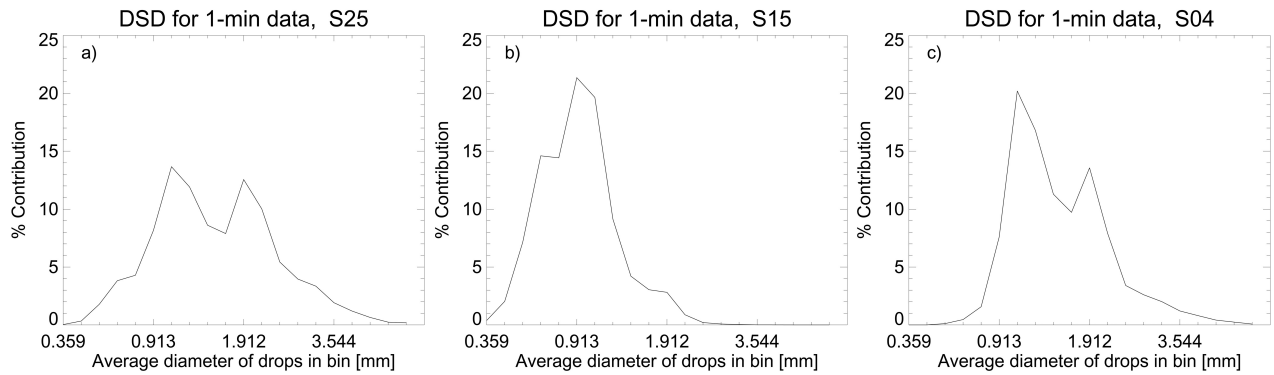


Figure 1 DSD histograms for each of the case studies a) barotropic b) weakly baroclinic c) strongly baroclinic environments.

Weakly Baroclinic: Storm S15 occurred in February 2005 and lasted 15 hr 18 min with a maximum rain rate of only 0.3 mmh^{-1} . This system occurred two days after a strong frontal passage (Table 2), so large temperature gradients were not present. However, a weak short-wave combined with low level advection of warm, moist Gulf air providing large-scale forcing resulting in steady widespread rain. Peak 1 dominates the DSD with a significantly diminished Peak 2, and Peak 3 is entirely absent, skewing the distribution strongly towards the smaller drops (Fig. 1b).

Strongly Baroclinic: Storm S04 occurred in December 2004 and lasted 4 hr 55 min with a maximum rain rate of 51.8 mmh^{-1} . This storm was associated with the passage of a cold front which created strong temperature gradients. The rain developed behind the front as the upper level low lagged the surface front. Peaks 1 and 2 in the DSD are pronounced as in the barotropic case, but the relative heights are more of a combination of the other two cases. There is also a

weak signal at Peak 3 and a longer tail at the upper end than the weakly baroclinic case.

The higher rain rates and tendency towards larger drops in the barotropic and strongly baroclinic cases allowed for the faster rate of rain accumulation indicated by the shorter storm durations. The weakly baroclinic case is characterized by a significantly lower rain rate and preference for smaller drops, explaining the relatively small rain accumulation for such a prolonged period of rain.

4.2 Seasonal Distribution

The distribution of baroclinicity categories by season (Table 1) demonstrates the trend throughout the course of a year. But are DSD variations consistent between seasonal and baroclinicity divisions? Figure 2 depicts the seasonally averaged histograms for the period of the study, which can be compared to the examples in Section 4.1 (Fig. 1).

In winter (Fig. 2b), the DSD most closely resembles the weakly baroclinic case (Fig. 1b), although the higher Peak 2 and longer tail in the seasonal distribution reflect the inclusion of strongly baroclinic storms (Table 1). Fall and spring DSDs (Figs. 2a,c) also resemble the weakly baroclinic case, but have an enhanced Peak 2 and longer tail representing contributions from barotropic storms (Table 1). The summer distribution (Fig. 2d) has a much more pronounced Peak 2 than during DJF and looks most similar to the strongly baroclinic case. However, this comparison reveals the confusion that can arise from ignoring the observed baroclinicity designation. Upon closer inspection, Peak 3 is enhanced compared to the other seasons, suggesting that this is indeed a reflection of averaged barotropic profiles and not a strongly baroclinic case study.

4.3 Baroclinicity Distribution

Averaging the storm distributions by the degree of baroclinicity of the environment shows that the three peaks remain discernible in each designation (Fig. 3). Although Peak 3 can only clearly be seen in the barotropic distribution, magnifying the tail portion of the profile reveals that the average DSD for all storms

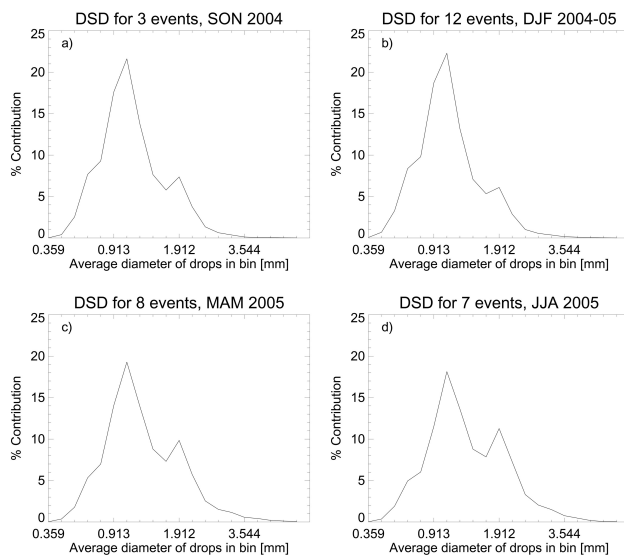


Figure 2 Seasonally averaged DSDs for a) fall 2004 b) winter 2004-05 c) spring 2005 d) summer 2005.

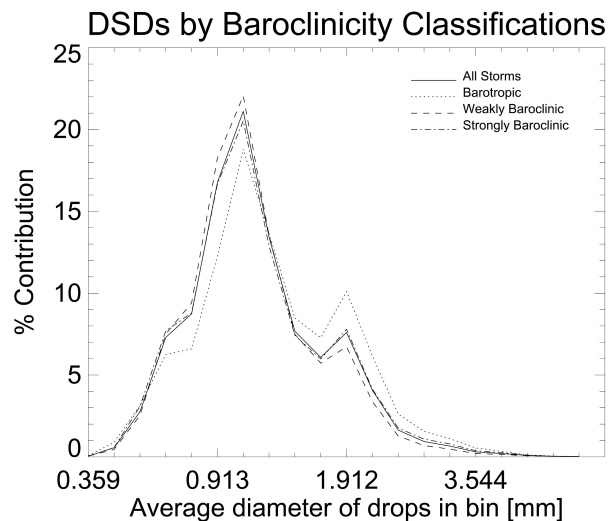


Figure 3 Averaged DSDs by baroclinicity designation for all storms.

contains that peak. As expected, the weakly baroclinic distribution exhibits the highest Peak 1, while the barotropic distribution has the most pronounced Peak 2. The gap between the barotropic distribution and other distributions at small diameters may indicate stronger evaporation or wind effects. The strongly baroclinic DSD closely approximates the averaged distribution over all storms suggesting that the strongly baroclinic systems more equitably distribute the microphysical burden of bin production.

5. DISCUSSION

Knowledge of how the drop-size distributions vary with the baroclinicity of the environment is important, but incomplete without an understanding of the microphysical processes generating the modes in the distributions. The mechanisms forming the droplets within the storms differ by type of storm (Steiner and Smith 1998), and more importantly between different baroclinicity regimes, represented by the varying heights of the peaks. Therefore relating the microphysical processes to the peaks allows for a more useful interpretation of the DSDs.

Peak 1 is the small drop mode, characteristic of weak to moderate convection. Weak updrafts in the convective core lead to the formation of small ice crystals that melt to create small rain drops.

Peak 2 is the medium drop mode, a feature of stratiform regions. Larger aggregates of ice crystals melt below the bright band region of mature mesoscale systems yielding an abundance of medium drops.

Peak 3 is the large drop mode, found only in the strongest convection where large graupel melts to form the largest drops.

Barotropic conditions are most prevalent in JJA, when convection is often thermally forced. Barotropic

conditions are also common in the transition seasons of MAM and SON. The storm DSDs associated with a barotropic environment skew toward large drops and higher magnitudes of Peak 2 and Peak 3. The microphysical characteristics associated with this DSD suggest periods of strong convection and robust stratiform rain regions.

Strongly baroclinic conditions are most common in DJF, when storms are often associated with cold frontal forcing. The storm DSDs in a strongly baroclinic environment have relatively less contribution from large drops compared to barotropic storms. Thus, one may expect relatively more weak to moderate convection and robust stratiform rain regions still contribute to rain production.

Weakly baroclinic conditions occur throughout the year, with the lowest occurrence in JJA. Warm frontal forcing is common during weakly baroclinic conditions and the storm DSDs show the least contribution from large drops. A predominance of weaker convection and warm frontal rain skews the distribution toward small drops and a larger Peak 1.

Multimodal distributions reflect the range of microphysical processes responsible for the observed raindrop spectra. Further, each of the storm types are climatologically important over Southeast Texas. Of the 30 identified storms, 14 were classified as weakly baroclinic, accounting for 252.8 mm (53.6%) of the total rain accumulated. Barotropic and strongly baroclinic represent 121.2 mm (25.7%) and 97.9 mm (20.7%), respectively. Since these storm types are present throughout the year (especially the weakly baroclinic storms), the importance of the storm classification is lost by partitioning the year by season.

Further investigation using radar techniques over the region will allow an increased understanding of the microphysical and dynamical processes within the mesoscale systems involved in the different degrees of environmental baroclinicity.

5. ACKNOWLEDGEMENTS

This work was supported by NSF grant ATM-0449782.

6. REFERENCES

- Smith, P.L., Z. Liu, and J. Joss, 1993: A study of the sampling-variability effects in raindrop size observations. *J. Appl. Meteo.*, **32**, 1259-1269.
- Steiner, M. and J.A. Smith, 2000: Reflectivity, rain rate, and kinetic energy flux relationships based on raindrop spectra. *J. Appl. Meteo.*, **39**, 1923-1940.
- _____, and _____, 1998: Convective versus stratiform rainfall: An ice-microphysical and kinematic conceptual model. *Atmos. Res.*, **47-48**, 317-326.
- _____, and A. Waldvogel, 1987: Peaks in raindrop size distributions. *J. Atmos. Sci., Notes and Correspondence*, **44**, 3127-3133.
- Waldvogel, A., 1974: The N_0 jump of raindrop spectra. *J. Atmos. Sci.*, **31**, 1067-1078.